International Journal of Technical Innovation in Modern Engineering & Science (IJTIMES)
Impact Factor: 3.45 (SJIF-2015), e-ISSN: 2455-2585
Volume 3, Issue 11, November-2017

Novel Control Strategy for Modular Multilevel Converter based Variable Speed PMSM Drive

K. DEEKSHITHA[1], Midde Mahesh[2]

[1]*M.Tech, Dept. of EEE, JNTUA, Ananthapuramu, A.P*
[1]*Kuchi.deeksha15@gmail.com*
[2]*M.Tech (Ph.D), Dept. Of EEE, JNTUACEA, Ananthapuramu, A.P*
[2]*mahesheee.midde@gmail.com*

Abstract—

This paper introduces a control conspire for the modular multilevel converter (MMC) to drive a variable-speed ac machine, particularly concentrating on enhancing dynamic execution. Hypothetically, the energy balance in the MMC cell capacitors is prone to be unstable at start-up and low-frequency operations. Also, the MMC topology basically requires propelled control procedures to balance energy and mitigate the voltage pulsation of every cell capacitor. This paper proposed a control system for the vigorous dynamic reaction of MMC even at zero output frequency utilizing leg offset voltage infusion. The leg offset voltage for balancing the arm energy is delivered by coordinate estimation without the circulating current control circle controller. The ac machine has been driven from stop to evaluated speed without intemperate cell capacitor voltage swells using the modern Fuzzy logic controller (FLC) is proposed methodology. The simulation outcomes check that steady operation and compare the outcomes is ensured down to <2% of the evaluated speed under 40% phase stack torque aggravation.

Keywords—Arm energy balancing, dynamic performance, modular multilevel converter, PMSM drive, fuzzy logic controller.

I. INTRODUCTION

AMODULAR multilevel converter (MMC) with concentrate on high-control medium voltage ac engine drives is exhibited [1]. The utilization of a MMC makes it conceivable to spare massive reactive parts in a medium-voltage engine drive application, for example, a line-transformer, harmonic filter, and dc-interface reactor. A contrasted and customary medium voltage source converter, the MMC has a measured structure made up of indistinguishable converter cells. Since it can undoubtedly give higher number of voltage level for medium voltage applications, the nature of the output voltage waveform is better. Likewise, due to the particular structure it has focal points, for example, simple support and get together.

Fig. 1 demonstrates the circuit arrangement of a MMC. This topology should be controlled by additional balancing methodologies. As appeared in Fig. 1, since the upper and lower arm currents move through cells in each arm, the relating arm currents cause major occasional pulsations of cell capacitor voltages. The voltage pulsation of every cell's capacitor is generally influenced by the output phase current and output frequency. Hypothetically, the extent of the cell voltage change is corresponding to size of the output phase current and conversely relative to working frequency [2]. Consequently, exceptional exertion is requested to drive the ac machine through MMC, which requires significant beginning torque and low-speed enduring state operation. In late investigations of [3], the standards and calculations for ac engine drives with the MMC have been presented. Notwithstanding, they didn't address the real control methodologies, for example, changing output frequency, including stop and covering load torque unsettling influence. The energy balancing control is one of the principle issues of MMC

framework. In numerous literary works [2], the energy balancing controls of a MMC that utilizations flowing current control and balance conspire have been presented. The leg offset voltage is utilized to direct the circulating current and has little impact on ac and dc terminal voltages. The traditional balancing controls require the flowing current controller that delivers the leg balance voltage reference from the contribution of coursing current references utilizing the proportional and integral (PI) or the corresponding and resonant controller.

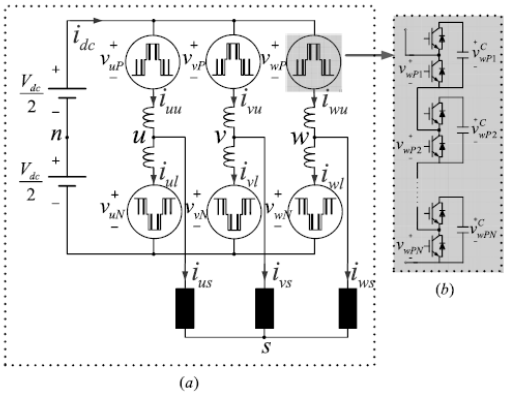

Fig. 1. Circuit configuration of the MMC.

The execution of the coursing current controller effectively affects the elements and many-sided quality of the balancing control. Along these lines, to enhance the balancing execution by expanding band width of the balancing controller, this paper proposes an balancing control strategy without the circulating current controller. Likewise, the distinction between the cell voltages can be decreased quicker. Therefore, from the point of view of the control elements and control multifaceted nature, the proposed leg offset voltage infusion technique is preferable and more straightforward over the traditional flowing current infusion strategy. Besides, the infusing frequency of leg offset voltage infusion strategy can be expanded more than that of current infusion technique, due to the broadened data transfer capacity of the proposed strategy. In this way, inferable from the high-frequency infusion with the proposed strategy, the variance of cell capacitor voltage can be limited contrasted and circulating current infusion technique.

The objective of this paper is to propose a fuzzy logic control (FLC) methodology of the whole frequency run operation including halt for variable speed air conditioning engine drive. The proposed strategy decreases the control execution corruption of the MMC when the load torque abruptly changes. The control conspire presents two operation modes: 1) a low-frequency mode for start-up and low-speed operation and 2) a typical frequency mode from medium to higher speed operation. The procedure in the low-frequency mode misuses leg offset voltage and regular mode voltage with the high-frequency part to suppress the cell capacitor voltage swell. The square wave voltage is utilized as the leg balance voltage, which demonstrates that the circulating current peak is lessened when contrasted and sinusoidal waveform of the voltage [3].

To demonstrate the adequacy of the proposed control procedures, a 12-kV 24-MVA MMC-based customizable motor drive framework was planned utilizing the PSIM programming. The reproduction results could offer the practicality and preferred standpoint of the contrived technique for high-control medium voltage drives with MMC. The examinations were led for looking at highlights of the sinusoidal and square wave leg offset voltage. The steady operation at 1 Hz, which is <2% of the appraised speed, is appeared under an unexpected advance load torque disturbances from 0% to 40% to exhibit the dynamic execution. The test comes about demonstrate that all control procedures was very much consolidated in the variable-speed ac motor drive framework with a load where the torque differs in corresponding to the square of the speed, similar to fans, blowers, or pumps.

II. CONFIGURATION AND BASIC PRINCIPLE OF THE MMC

Fig. 1(a) demonstrates the circuit arrangement of the MMC. The three-phase MMC is made out of three legs and every leg has two arms and two arm inductors. Each arm has fell N-indistinguishable half-connect circuit-based cells, and every cell comprises of one dc capacitor and two dynamic switching devices. The fell cell modules are appeared in Fig. 1(b) in detail. In Fig. 1(a), i_{xu} and i_{xl} are the upper and lower arm currents, separately, and i_{xS} is the output phase current where x' speaks to the u-, v-, or w-phase. The output phase current, i_{xs}, and circulating current, i_{xO}, are figured from the upper and lower arm currents depicted in (1) and (2). Along these lines, the arm currents can be reasoned as (3) and (4), as indicated by the decoupled control plot in [4]-[5]

$$i_{xs} = i_{xu} - i_{x1} \quad (1)$$

$$i_{xo} = \frac{(i_{xu} + i_{x1})}{2} \quad (2)$$

$$i_{xu} = \frac{1}{2} i_{xs} + i_{xo} \quad (3)$$

$$i_{x1} = -\frac{1}{2} i_{xs} + i_{xo} \quad (4)$$

The leg balance voltage, v_{xo}, produces a flowing current characterized as (5), where R and L remain for the protection and inductance of an arm inductor when all arm inductors in MMC are thought to be indistinguishable. From the voltage connections along the x-phase circle, the upper, and lower arm voltage references are meant as (6) and (7), separately, where V_{dc} is the dc-interface voltage, and V_{xP} and V_{xN} are the upper and lower arm voltages, individually. The basic mode voltage, v_{sn}, is the voltage distinction between hubs s' and n', and v_{xs} is the phase voltage, which is v_{xs} = Vmcos(ωst). A detaile numerical portrayal of the connections in a MMC is given in [5]

$$v_{xo} = \left(R + L\frac{d}{dx}\right) i_{xo} \quad (5)$$

$$v_{xP}^* = \frac{V_{dc}}{2} - v_{xs}^* - v_{sn}^* - v_{xo}^* \quad (6)$$

$$v_{xN}^* = \frac{V_{dc}}{2} + v_{xs}^* + v_{sn}^* + v_{xo}^* \quad (7)$$

The quick energy of each arm in the x-phase can be derived as (8) and (9). These two conditions must be considered to comprehend of the proposed balancing control

$$P_{xP} = v_{xP}^* i_{xu} = \left(\frac{V_{dc}}{2} - v_{xs}^* - v_{sn}^* - v_{xo}^*\right)\left(\frac{1}{2} i_{xs} + i_{xo}\right) \quad (8)$$

$$P_{xN} = v_{xN}^* i_{x1} = \left(\frac{V_{dc}}{2} + v_{xs}^* + v_{sn}^* - v_{xo}^*\right)\left(-\frac{1}{2} i_{xs} + i_{xo}\right) \quad (9)$$

What's more, the upper and lower arm energy can be ascertained by (10) and (11), individually. Each arm energy is the whole of the cell capacitor energies in the relating arm at x-phase leg

$$E_{xp} = \frac{1}{2} C_{cell} \sum_{i=1}^{N} (v_{xPi}^C)^2 \quad (10)$$

$$E_{xN} = \frac{1}{2} C_{cell} \sum_{i=1}^{N} (v_{xNi}^C)^2 \quad (11)$$

III. PROPOSED BALANCING CONTROL SCHEME

A. Start-Up and Low Frequency Mode

The capacitor control contrast between the upper and lower arm, which is determined as (12) from (8) and (9), influences the cell capacitor voltage balance of the arms. The initial two terms on the right-hand side in (12), $0.5V_{dc} i_{xs} - 2v_{xs}^* i_{xo}$, have impressive dc or low-frequency segments. Hence, when the output frequency is dc or low, the voltage contrast between the arms will veer because of this low frequency term

$$P_{xP} - P_{xN} = 0.5V_{dc} i_{xs} - 2v_{xs}^* i_{xo} - 2v_{sn}^* i_{xo} - v_{xo}^* i_{xs} \quad (12)$$

To balance the power contrast between arms, a control system abusing the normal mode voltage, v_{sn}, was utilized as a part of this paper. The normal mode voltage can be viewed as an extra level of flexibility for controllability since the regular mode voltage does not influence the line-to-line output voltage. It is normal to choose the frequency of the basic mode voltage as a high frequency to limit the cell capacitor voltage vacillations. Henceforth, the third term on the right-hand side in (12), $2v_{sn}^* i_{xo}$ can be utilized to balance the energy of arms with the high frequency parts in v_{sn} and i_{xo}. For accommodation, the low-and high-frequency components can be isolated from i_{xo} and v_{sn} as (13) and (14), where ~ and ^ allude to the low and high-frequency segments, separately

$$i_{xo} = \tilde{\imath}_{xo} + \hat{\imath}_{xo} \quad (13)$$

$$v_{sn} = \hat{v}_{sn} \quad (14)$$

The power contrast between the upper and lower arms can be modified from (12) to (14), and after that, the low-frequency control segment can be separated as in (15). Here, the power contrast ought to be controlled as invalid

$$(P_{xP} - P_{xN})|_{low\ freq} \approx 0.5V_{dc} i_{xs} - 2v_{xs}^* \tilde{\imath}_{xo} - 2\hat{v}_{sn}^* \hat{\imath}_{xo}^* |_{low\ freq} = 0 \quad (15)$$

To invalidate the low-frequency part as in (15), the low-frequency segment of $2v_{xs}^* \tilde{\imath}_{xo}$ ought to be controlled. Accordingly, $\hat{v}_{sn}^*$ and $\hat{\imath}_{xo}^*$ ought to be controlled as a similar highfrequency, to influence the ability to term of $2\hat{v}_{sn}^* \hat{\imath}_{xo}^*$ have dc or lowfrequency segment. On account of the sinusoidal leg balance voltage infusion technique, $\hat{v}_{sn}^*$ and $\hat{v}_{xo}^*$ can be characterized as (16) and (17), and ωh alludes to the precise speed of the high-frequency segment, v_{sv} for the successful estimation of normal mode voltage, and $\hat{v}_{xo}$ for the greatness of high-frequency leg offset voltage, which may have dc and a few low-frequency parts

$$\hat{v}_{sn}^* = \sqrt{2} V_{sn} cos(\omega_h t) \quad (16)$$

$$\hat{v}_{sn}^* = \tilde{V}_{xo} \cos(\omega_h t + \emptyset) \quad (17)$$

The phase angle φ in (17) between the leg offset voltage and flowing current is gotten from (18) to influence the coursing current to synchronize with the normal mode voltage

$$\emptyset = arctan\left(\frac{\omega_h L}{R}\right) \quad (18)$$

All in all, $\omega_h L$ is considerably bigger than R, in light of the fact that the frequency of infusing voltage is very high. In any case, if the frequency isn't sufficiently high and the arm protection can't be overlooked, the arm impedance parameters would should be recognized. For distinguishing proof, at the framework dispatching phase, the non interacting leg offset voltage can be infused into the arm, and the circulating current could be fed back as in (5). Subsequently, the phase point between the leg offset voltage and the flowing current in (18) can be acquired. Under the presumption of R_ωh L, φ is roughly π/2. From (5), (16) and (17), the low-frequency segment of the power related with the regular mode voltage and the circulating current can be determined as (19) utilizing the leg offset voltage, where p speaks to a differential administrator

$$2\hat{v}_{sn} \hat{\imath}_{xo}|_{low\ freq} \approx 2\hat{v}_{sn} \frac{\hat{v}_{xo}}{pL}\Big|_{low\ freq}$$

$$= \frac{2\sqrt{2} V_{sn} \tilde{V}_{xo}}{\omega_h L} \cos(\omega_h t) \sin\left(\omega_h t + \frac{\pi}{2}\right)\Big|_{low\ freq}$$

$$= \frac{2\sqrt{2}V_{sn}\tilde{V}_{xo}}{\omega_h L}\left(\frac{1}{2}sin\left(\frac{\pi}{2}\right)+\frac{1}{2}sin\left(2\omega_h+\frac{\pi}{2}\right)\right)\Big|_{low\ freq}$$

$$= \frac{\sqrt{2}V_{sn}\tilde{V}_{xo}}{\omega_h L}. \quad (19)$$

And then, $2\hat{v}_{sn}^{*}\hat{\imath}_{xo}^{*}$ in (15) can be substituted with (19). The magnitude of high-frequency leg offset voltage, $\tilde{V}_{xo}$, can be calculated as

$$\frac{\sqrt{2}V_{sn}\tilde{V}_{xo}}{\omega_h L} \approx \frac{1}{2}V_{dc}\,i_{xs} - 2v_{xs}^{*}\tilde{\imath}_{xo}$$

$$\tilde{v}_{xo} \approx \frac{\omega_h L}{\sqrt{2}V_{sn}}\left(\frac{1}{2}V_{dc}\,i_{xs} - 2v_{xs}^{*}\tilde{\imath}_{xo}\right) \quad (20)$$

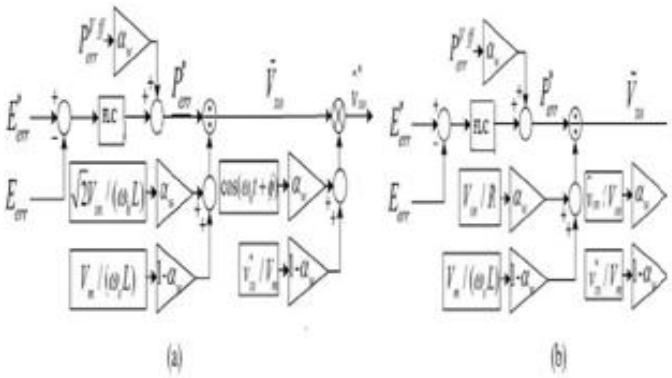

Fig. 2. Proposed control scheme for variable-speed PMSM drives using FLC. (a) Sinusoidal wave voltage injection method. (b) Square wave voltage injection method. αW is weighting factor for switchover, which is described in Section III-C.

For the situation that the sinusoidal wave voltage is infused to both the normal mode and the leg balance voltage, the balancing control methodology is appeared as a square graph in Fig. 2(a). E_{err} is the energy contrast between the upper and lower arms as in (21). E∗ fail is the reference of energy contrast and ought to be set as invalid to keep the balance of the arm energies

$$E_{err} = E_{xp} - E_{xN} = \frac{1}{2}C_{cell}\{\sum_{i=1}^{N}(v_{xPi}^{C})^2 - \sum_{i=1}^{N}(v_{xNi}^{C})^2\} \quad (21)$$

P_{leg}^{vff} in Fig. 2(a) can be derived as (22) by (20)

$$P_{err}^{Vff} = \frac{1}{2}V_{dc}\,i_{xs} - 2v_{xs}^{*}\tilde{\imath}_{xo} \quad (22)$$

On account of the square leg balance voltage infusion, then again, the square wave voltage can be infused to both the regular mode and the leg offset voltage as appeared in Fig. 2(b). For this situation, ˆ v∗ sn can be characterized by (23) and fh remains for the frequency of the infused high-frequency voltage

$$\hat{v}_{sn}^{*} = \begin{cases} -V_{sn} & \left(0 \le t < \frac{1}{2f_h}\right) \\ V_{sn} & \left(\frac{1}{2f_h} \le t < \frac{1}{f_h}\right) \end{cases} \quad (23)$$

Under the presumption that the arm protection, R, is overwhelming amid each given quasi steady half period, $\frac{1}{2f_h}$), $\hat{v}_{xo}^{*}$ can be approximated as (24) from (5), (15), and (23)

$$\hat{v}_{xo}^{*} \approx \begin{cases} -\frac{R}{2V_{sn}}\left(\frac{1}{2}V_{dc}\,i_{xs} - 2v_{xs}^{*}\tilde{\imath}_{xo}\right) & \left(0 \le t < \frac{1}{2f_h}\right) \\ \frac{R}{2V_{sn}}\left(\frac{1}{2}V_{dc}\,i_{xs} - 2v_{xs}^{*}\tilde{\imath}_{xo}\right) & \left(\frac{1}{2f_h} \le t < \frac{1}{f_h}\right) \end{cases} \quad (24)$$

P^{Vff} blunder in Fig. 2(b) can likewise be gotten from (22) utilizing (24) comparatively with the instance of sinusoidal wave.

B. Normal Frequency Mode

Since the output frequency is sufficiently high in the ordinary frequency mode, the voltage change of the cell capacitor is decent. In this mode, the coursing current is controlled to have just dc segment to limit the conduction misfortune caused by the extra flowing current. As the operation frequency builds, in the mean time, the edge of the regular mode voltage diminishes. Subsequently, the basic mode voltage is less accessible for balancing control.

Functional MMC frameworks may have a natural unbalance because of slight asymmetries in cells, auxiliary blunders, and different issues.

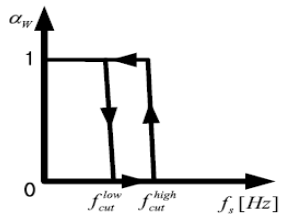

Fig. 3 Relationship between operating frequency and weighting factor

In ordinary frequency mode, in this manner, it ought to be performed just to dispense with the unavoidable little dc unbalances. The balancing can be accomplished utilizing the coursing present as 2v∗xsixo in (12). By controlling the leg balance voltage for coursing current to have key frequency part, this dc unbalance can be smothered.

C. Switchover Between Two Modes

As said already, as the high-frequency parts of the regular mode and leg offset voltage are just infused in low-working frequency modes, the leg balance voltage reference changes relying upon the output frequency of MMC. A switchover strategy between the low-and high-frequency modes appeared in Fig. 3 is formulated by the weighting factor, αW. What's more, this factor is connected to the switchover of the balancing control conspire appeared in Fig. 2. What's more, the strategy would have the hysteresis band to avoid gabbing in the region of the switchover frequency, fcut.

IV. OVERALL CONTROL SCHEME FOR ENTIRE FREQUENCY OPERATION

Fig. 4 demonstrates the general controller for the whole frequency operation from stop to typical frequency mode. To start with, the averaging controller completes directing the leg control, which is the distinction between dc-connect input power and air conditioning output control. The leg control is ascertained as (25) by including (8) and (9)

$$P_{xP} + P_{xN} \approx V_{dc}\,\tilde{\imath}_{xo} - 2v_{xo}^{*}\,\hat{\imath}_{xo} - v_{xs}^{*}\,i_{xs} - \hat{v}_{sn}^{*}\,i_{xs} \quad (25)$$

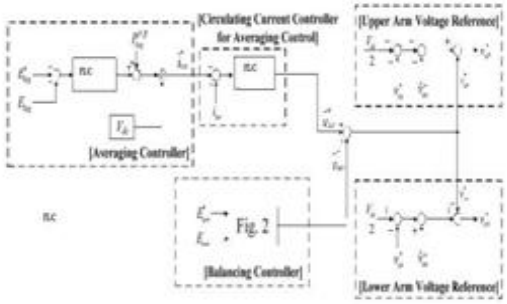

Fig. 4. Proposed overall control scheme for variable-speed PMSM drives using fuzzy logic controller.

Since the low-frequency control segment in (25) ought to be invalidated as in (26), the controller output has dc and second order consonant frequency parts as depicted in (27)

$$P_{xP} + P_{xN}|_{low\ freq} \approx V_{dc}\,\tilde{\imath}_{xo}^{*} - v_{xs}^{*}\,i_{xs} = 0 \quad (26)$$

$$\tilde{\imath}_{xo}^{*} = v_{xs}^{*}\,i_{xs}/V_{dc} \quad (27)$$

E_{leg} is the energy of the leg and it can be computed as (28). E_{leg}^{*} is the reference energy of the leg as (29), where v_c^{*} is the reference estimation of cell capacitor voltage, V_{dc}/N

$$E_{leg} = E_{xP} + E_{xN} = \frac{1}{2}C_{cell}\{\sum_{i=1}^{N}(v_{xPi}^{C})^2 + \sum_{i=1}^{N}(v_{xNi}^{C})^2\} \quad (28)$$

$$E_{leg}^{*} = \frac{1}{2}\frac{C_{cell}}{2N}4N^2v_c^{*2} = NC_{cell}\,v_c^{*2} \quad (29)$$

The bolster sending power term, P_{leg}^{vff}, can be gotten as $v_{xs}^{*}\,i_{xs}$ from (27). In this way, the PI controller can just be received as the flowing current controller for the averaging control. The insights about the averaging controller are depicted in [10]. In the interim, the balancing controller can be picked between two plans in Fig. 2 that are to be specific, the sinusoidal and the square wave voltage infusions. As appeared in Fig. 4, the balancing controller straightforwardly influences the leg to balance voltage without the flowing current controller to dispose of the energy contrast amongst upper and lower arms. By reason of this reality, the balancing controller has a more extensive data transmission, and can accomplish a superior transient reaction contrasted and the control conspire in light of the internal circulating current direction circle. At long last, the upper and lower arm voltage references are blended as (6) and (7), which are made out of v_{xs}^{*} from the output of phase current controller, v_{xo}^{*} from the averaging and balancing controller, and the infused normal mode voltage of $\hat{v}_{sn}^{*}$.

V. FUZZY LOGIC CONTROL (FLC)

Fuzzy rational is a type of numerous esteemed rationales in which reality estimations of variables might be any genuine number somewhere around 0 and 1. By differentiation, in Boolean rationale, reality estimations of variables may just be 0 or 1. Fuzzy rationale has been stretched out to handle the idea of halfway truth, where reality quality may extend between totally genuine and totally false. Besides, when etymological variables are utilized, these degrees might be overseen by particular capacities.

Normally fuzzy rational control framework is made from four noteworthy components exhibited on Figure fuzzification interface, fuzzy induction motor, fluffy principle grid and defuzzification interface. Every part alongside fundamental fuzzy rationale operations will be depicted in more detail below

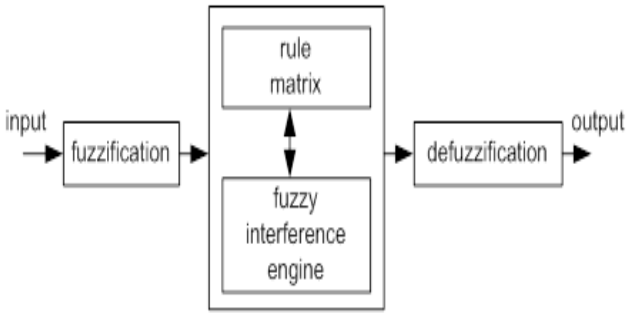

. Fig.5 Fuzzy logic interface system.

The fuzzy rational investigation and control strategies appeared in Fig. 1 can be depicted as:

1. Receiving one or expansive number of estimations or other appraisal of conditions existing in some system that will be dissected or controlled.
2. Processing all got inputs as indicated by human based, fuzzy "assuming then" standards, which can be communicated in basic dialect words, and consolidated with conventional non-fuzzy preparing.
3. Averaging and weighting the outcomes from all the individual principles into one single output choice or sign which chooses what to do or advises a controlled system what to do. The outcome output sign is an exact defuzzified esteem. First of all, the different level of output (high speed, low speed etc.) of the platform is defined by specifying the membership functions for the fuzzy sets.

Table 1: Fuzzy Rules

Change in error	Error						
	Nb	nm	Ns	zr	ps	pm	Pb
Nb	Nb	nb	Nb	nm	nm	Ns	Zr
Nm	Nb	nb	Nm	nm	ns	Zr	Ps
Ns	Nb	nm	Nm	ns	zr	Ps	Pm
Zr	Nm	nm	Ns	zr	ps	pm	Pm
Ps	Nm	ns	Zr	ps	pm	pm	Pb
Pm	Ns	zr	Ps	pm	pm	pb	Pb
Pb	Zr	ps	Pm	pm	pb	pb	Pb

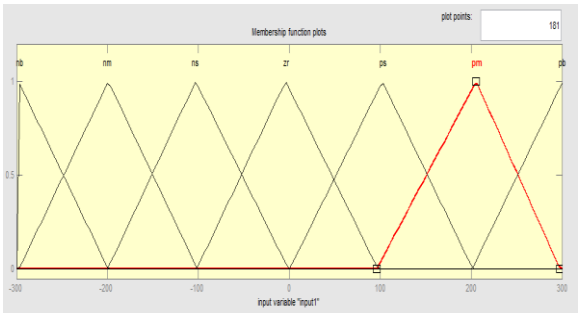

(a)

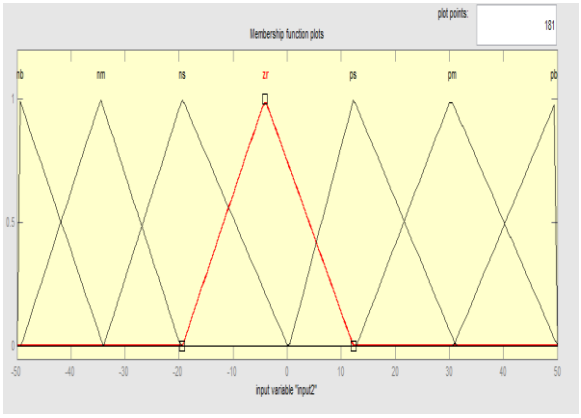

(b)

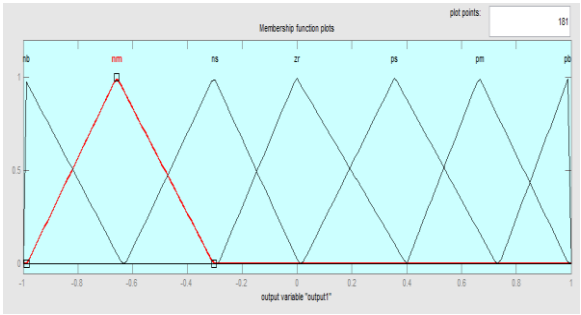

(c)

Fig.6. Membership functions: (a) Input1, (b) Input2, (c) output1

VI. SIMULATION RESULTS

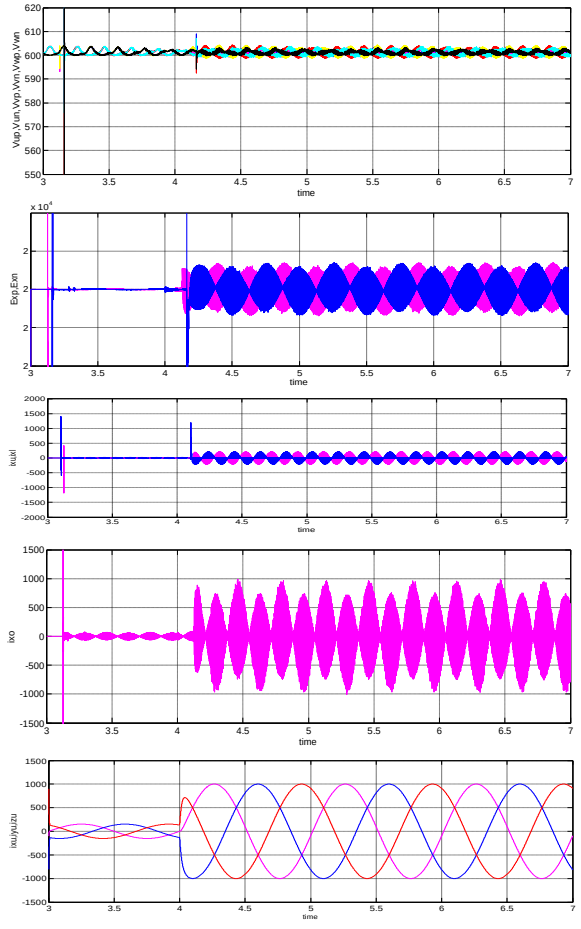

(a)

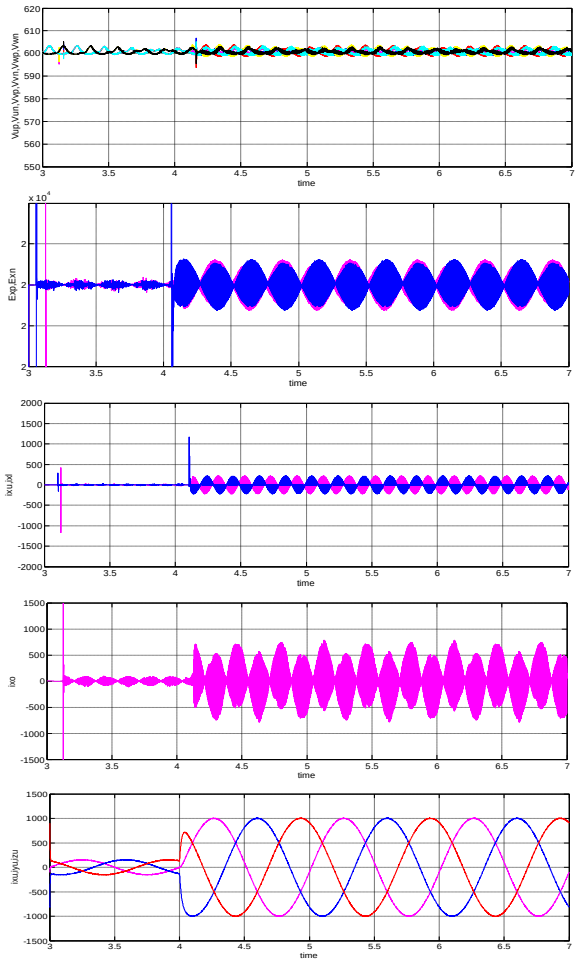

(b)

Fig.7. Simulation waveform when applying the proposed leg offset voltage injection method with 6r/min speed and step load torque from 10% to 40% of the rated torque using PI controller. (a) Sinusoidal waveform offset voltage injection.

(b) Square waveform offset voltage injection.

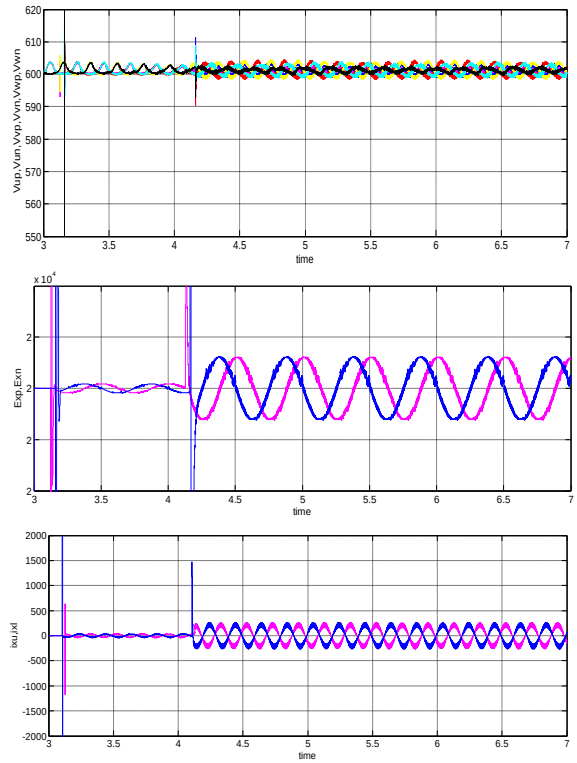

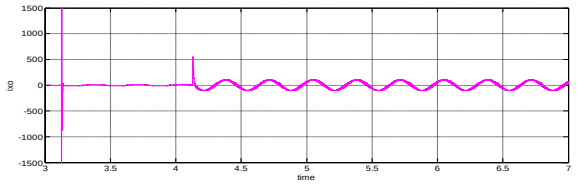
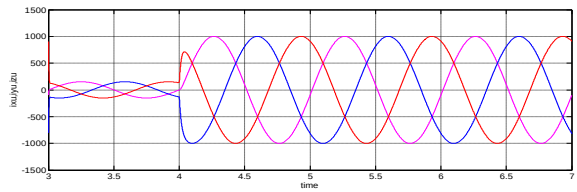

(a)

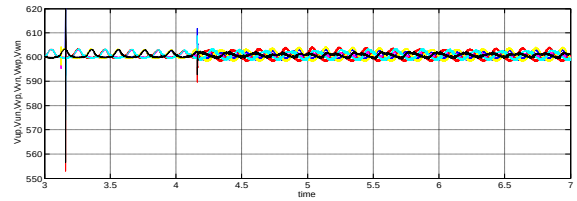
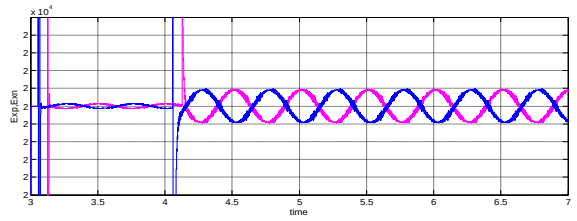
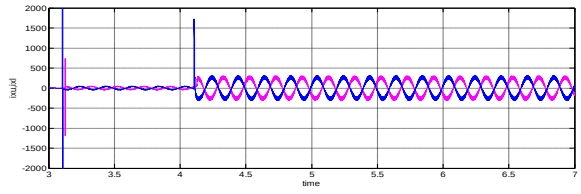
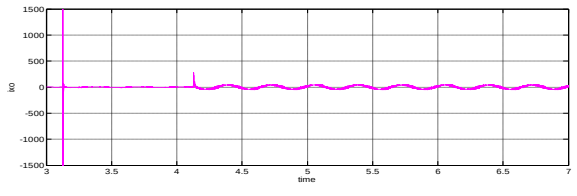
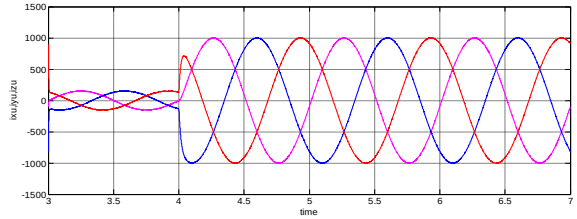

(b)

Fig.8. Simulation waveform when applying the proposed leg offset voltage injection method using fuzzy logic controller (a) Sinusoidal waveform offset voltage injection. (b) Square waveform offset voltage injection.

VII. CONCLUSION

In this paper, a control system for variable-speed ac motor drives in view of MMC has been displayed. To conquer the troubles of the power balance amongst cells and arms of MMC over wide operation speed extends, an immediate leg offset voltage infusion strategy has been formulated. Using the proposed Fuzzy logic controller strategy, the swell voltage of every cell of MMC has been kept inside suitable limits under the sudden utilization of 40% of appraised load torque at to a great degree low frequency, 1 Hz, which is <2% of evaluated frequency. In view of the simulation and test comes about, it can be noticed that the control execution of the upper and lower arm energy swell by the proposed leg balance voltage infusion technique is superior to that by the regular circulating current infusion strategy with the inward circle.

REFERENCES

[1] A. Lesnicar and R. Marquardt, "An innovative modular multilevel converter topology suitable for a wide power range," in *Proc. IEEE Power Tech Conf.*, Bologna, Italy, Jun. 2003.

[2] M. Hagiwara, K. Nishimura, and H. Akagi, "A medium-voltage motor drive with a modular multilevel PWM inverter," *IEEE Trans. Power Electron.*, vol. 25, no. 7, pp. 1786–1799, Jul. 2010.

[3] M. Hagiwara, I. Hasegawa, and H. Akagi, "Start-up and low-speed operation of an electric motor driven by a modular multilevel cascade inverter," *IEEE Trans. Ind. Appl.*, vol. 49, no. 4, pp. 1556–1565, Jul./Aug. 2013.

[4] J. Kolb, F. Kammerer, and M. Braun, "Straight forward vector control of the modular multilevel converter for feeding three-phase machines over their complete frequency range," in *Proc. 37th Annu. Conf. IEEE Ind. Electron. Soc. IECON*, Nov. 2011, pp. 1596–1601.

[5] J.-J. Jung, H.-J. Lee, and S.-K. Sul, "Control of the modular multilevel converter for variable-speed drives," in *Proc. IEEE Int. Conf. PEDES*, Dec. 2012, pp. 1–6.